ZIBELINE INTERNATIONAL™ PUBLISHING

Acta Chemica Malaysia (ACMY)

DOI: http://doi.org/10.26480/acmy.01.2024.46.50

ISSN: 2576-6724 (Print)
ISSN: 2576-6732 (Online)
CODEN: ACMCCG

RESEARCH ARTICLE

EFFECT OF SURFACTANT ON THE SYNTHESIS METHOD OF CU_2O-CU HETEROSTRUCTURE

Huajun Yao*, Ji Deng, Fangfang Xiao, Bo Ma, Maohui Li

School of Materials Science and Engineering, North Minzu University, Yinchuan, 750021, China.
Corresponding author email: 256474003@qq.com

ARTICLE DETAILS

Article History:

Received 23 June 2024
Revised 09 July 2024
Accepted 15 August 2024
Available online 19 August 2024

ABSTRACT

Heterostructure nanoparticles have excellent photoelectrochemical properties, because of the difference of heterostructure characteristics will greatly affect the performance of the play. Therefore, the selective growth of heterostructure nanoparticles is an important research content in the design and synthesis of advanced materials. In this thesis, the octahedral Cu_2O crystal was used as the research object. By adjusting the reaction time and the kind and quantity of Surfactant, the nucleation and growth mode of Cu nanoparticles can be different. So that, Cu nanocrystals can be grown in situ at different positions such as the edges and faces of the octahedral Cu_2O, and the Cu_2O-Cu heterostructures with different spatial configurations were precisely constructed. The results showed that the content of Cu particles on the Cu_2O surface also increased with the increase of reaction time. The addition of surfactant PVP hinders the in-situ growth of Cu nanoparticles on the Cu_2O surface edge. The addition of CTAB can increase the particle size of Cu nanoparticles. And the addition of SDS can reduce the particle size of Cu nanoparticles while preferentially growing and aggregating on the octahedral Cu_2O edge.

KEYWORDS

Surfactant, cuprous oxide, heterostructure, in-situ reduction

1. INTRODUCTION

Photocatalysis is a complex process involving steps such as photo trapping, charge separation, and molecular adsorption activation (Chachvalvutikul et al., 2021; Li et al., 2024; Gore et al., 2024). The light absorption efficiency and band gap width of photocatalytic materials are crucial in water-catalyzed reactions (Abd-Elkader and Deraz, 2013; Murzin, 2023; Badry et al., 2024). However, due to the limitation of band gap width and other factors, pure semiconductor catalytic materials cannot respond to the broad spectrum of sunlight, and the photon yield is low (Balakrishnan et al., 2024; Liyanaarachchi and Fernando, 2013; Xiong et al., 2011). Therefore, Cu2O needs to be combined with metal materials to form heterostructure particles (Kociołek-Balawejder et al., 2023; Hamdani and Bhaskarwar, 2022).

Nowadays, the photocatalytic efficiency of M-Cu2O heterostructures has a large gap compared with the theoretical efficiency, and the performance improvement space is large (Malik et al., 2024; Özdal and Kavak, 2020; Kempasiddaiah et al., 2024). The energy state of different positions of the crystal is different from the energy state of the particle size (Zhao et al., 2023; Mani et al., 2009). Current studies often unify these variables, thus ignoring the influence of the check point and particle size on the photocatalytic performance (Choi and Yoon, 2022; Javaid et al., 2015; Yoon et al., 2022; Uthirakumar et al., 2024). Therefore, this study uses surfactants to prepare Cu2O-Cu heterostructure nanoparticles with different surface characteristics, and then it is necessary to clarify the influence of different check points and particle sizes on the photocatalytic performance.

In this paper, the octahedral Cu2O particles are used as the research object, the appropriate preparation method is selected, and the nucleation and growth mode of nano-Cu particles on the surface of Cu2O are changed by regulating the reaction time and the type and quality of surfactants. The in-situ growth of nano-Cu crystals at different positions such as the edges and planes of Cu2O polyhedral is realized, and the precise construction of Cu2O-Cu heterostructures with different surface characteristics is completed. At the same time, the phase of the product is characterized by XRD test, and the particle size, morphology and structure of M-Cu2O heterostructures are characterized and analyzed by SEM. Finally, the influence of various surfactants on Cu2O-Cu heterostructures is clarified.

2. EXPERIMENT

2.1 Experimental raw materials and reagents

The reagents used in the experiment are: copper sulfate pentahydrate (CuSO4·5H2O), sodium hydroxide (NaOH), glucose (C6H12O6), ethylene glycol (HOCH2CH2OH), anhydrous ethanol (CH3CH2OH), hydroquinone (C6H6O2), polyvinylpyrrolidone (C6H9NO) n, sodium dodecyl sulfate (C12H25O4NaS), cetyltrimethylammonium bromide (C19H42BrN). The drugs used are all analytically pure and purchased from Shanghai search banner Reagent Co., Ltd.

2.2 Preparation method

First prepare Cu2O powder: place the copper sulfate solution (0.4994 g/30 ml) in a water bath and heat it to 55 °C, then slowly drop in the NaOH solution (6.8 g/25 ml) after heating; after 5 mins, add 0.5 g of hydroquinone powder and continue to react for 1h; the powder of the mixed solution is centrifuged for multiple times and then used for standby.

Then the dried Cu2O powder was weighed 20 mg into a conical flask filled with 30 ml of ethylene glycol, and the surfactant was not added,

Quick Response Code	Access this article online	
	Website: www.actachemicamalaysia.com	**DOI:** 10.26480/acmy.01.2024.46.50

Cite the Article: Huajun Yao, Ji Deng, Fangfang Xiao, Bo Ma, Maohui Li (2024). Effect of Surfactant on The Synthesis Method of Cu_2O-Cu Heterostructure. *Acta Chemica Malaysia, 8(1): 46-50.*

respectively, and PVP, CTAB, and SDS were added. After heating, add NaOH solution (2 g/10 ml); after 5 mins, pour glucose solution (1.98 g/10 ml) to obtain the desired sample.

2.3 Test method

The morphology and structure of the samples were characterized by scanning field emission scanning electron microscopy (SEM), and the phase analysis was carried out by X-ray diffraction (XRD).

3. Results and Analysis

3.1 Characterization of octahedral Cu2O and Cu2O-Cu heterostructures

From the SEM diagram of Figure 1, it can be seen that the octahedral Cu2O exposes the (111) crystal plane, the particle size is about 4 μm, and the surface is very smooth with almost no impurities.

In the XRD shown in Figure 2, strong diffraction spikes appear at 2θ = 36.42 °, 42.31 °, 61.37 °, 3.52 °, 77.37 °, and their corresponding crystal planes are (110), (111), (200), (220), (311), respectively (Ma et al., 2018). In addition, no other impurity diffraction peaks appear, indicating that only Cu2O is generated during the sample preparation process. It is worth noting that the strongest diffraction peak is the (111) crystal plane, which is consistent with the growth crystal plane in Figure 1.

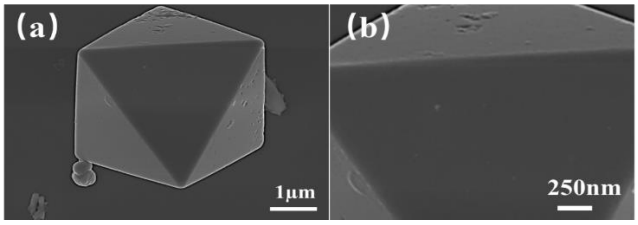

Figure 1: SEM images of octahedral Cu2O: (a) low-power SEM images, (b) high-power SEM images

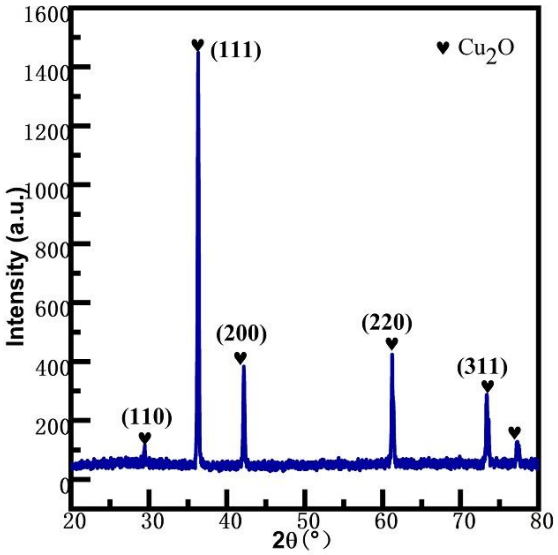

Figure 2: XRD diagram of octahedral Cu2O reacted at 55 °C for 60 mins

Using the reductivity of glucose, monovalent Cu is reduced to zero-valent Cu, and then Cu nanoparticles are reduced in situ on the surface of Cu2O particles. The octahedral Cu2O-Cu heterostructure shown in Figure 3 still maintains the intact octahedral structure, and uniformly dispersed particles appear on the surface of Cu2O. After 10 mins of reaction, many Cu nanoparticles appeared on the surface of Cu2O particles, but the surface of Cu2O was not yet dense. After 30 mins and 60 mins of reaction, the Cu nanoparticles on the surface of Cu2O particles have been dense, forming a core-shell structure.

As shown in Figure 4, the diffraction peaks of Cu2O appear in four places at 2θ = 36.42 °, 42.31 °, 61.37 °, 73.52 °, and Cu diffraction peaks appear at 2θ = 43.30 °, 50.43 °, 74.13 °, indicating that the small particles on the surface of the octahedral Cu2O particles are Cu nanoparticles (Ma et al., 2018).

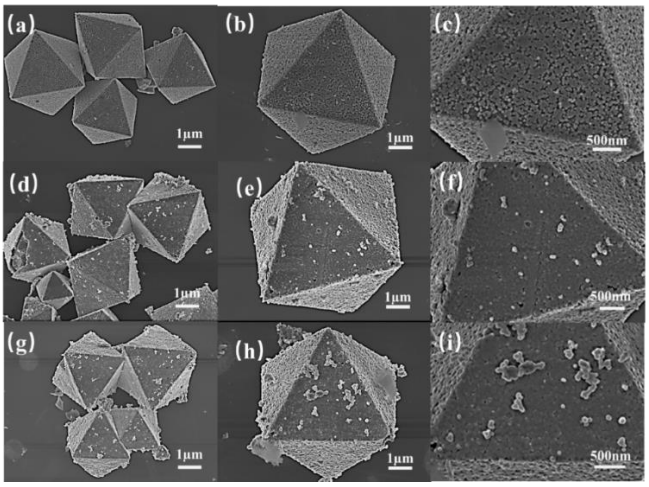

Figure 3: SEM diagrams of the octahedral Cu2O-Cu heterostructure: (a-c) reaction for 10 mins, (d-f) reaction for 30 mins, (g-i) reaction for 60 mins

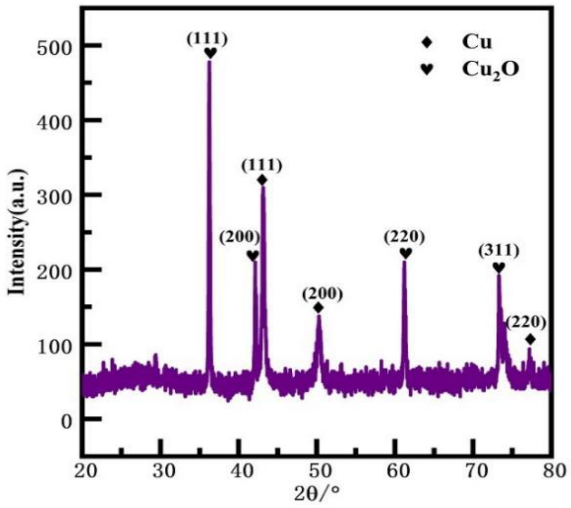

Figure 4: XRD diagram of octahedral Cu2O-Cu heterostructures reacted at 60 °C for 60 mins

3.2 Effect of PVP on Cu2O-Cu heterostructures

As shown in Figure 5, a surfactant of 0.1 g of PVP was added, and when the reaction time was controlled for 10 mins, it can be seen from Figure 5 (a-c) that there are many nano-Cu particles on the (111) crystal plane of Cu2O-Cu heterostructure, but they are not completely wrapped, and there are some small gaps on the surface of Cu2O; then continue the reaction to 30 mins, and Figure 5 (d-f) shows that after the reaction of Cu2O-Cu heterostructure for 30 mins, the Cu nanoparticles on the surface of its Cu2O particles have become denser than that of 10 mins, and the small gaps on the surface of the 7Cu2O particles become smaller, indicating that the Cu nanoparticles on the surface of Cu2O nanoparticles continue to form at this time, but they are not completely dense; with the further increase of time to 60 mins, the Cu2O-Cu heterostructure is further increased, as shown in Figure 5. As shown by (g-i), the Cu nanoparticles on the surface of its Cu2O particles grow more, so that the surface of its Cu2O particles has been completely dense.

As shown in Figure 6 and Figure 7, after adding 0.5 g and 1.0 g of PVP, there were Cu nanoparticles on the (111) crystal plane of Cu2O in the Cu2O-Cu heterostructure sample at 10 mins, but the number of distributions was reduced compared with before, and there was almost no growth at the edges. Then the reaction continued to 30 mins and 60 mins, and it was more obvious that there was no distribution of Cu nanoparticles at the edges. Therefore, for the octahedral Cu2O particles, the addition of PVP plays a role in the position of the edges, which will hinder the in-situ reduction of Cu2O to Cu nanoparticles at the position of the octahedral Cu2O edges.

As shown in Figure 8, the XRD diffraction peak did not change significantly after the addition of PVP, indicating that the addition of surfactant PVP did not generate new substances, and still reduced Cu2O to Cu nanoparticles in situ.

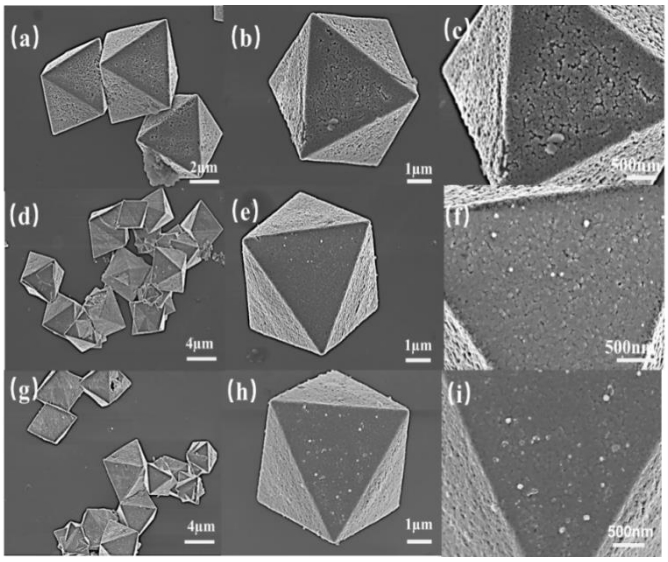

Figure 5: SEM images of Cu2O-Cu heterostructure particles prepared by adding 0.1 g PVP: (a-c) reaction for 10 mins, (d-f) reaction for 30 mins, (g-i) reaction for 60 mins

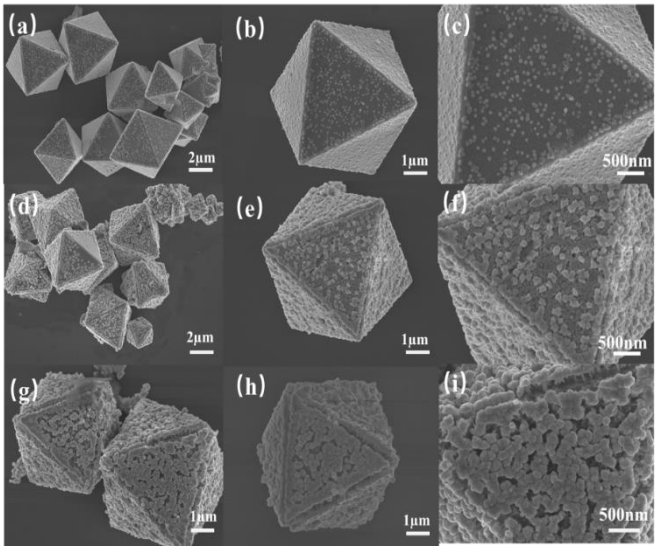

Figure 6: SEM images of Cu2O-Cu heterostructures prepared by adding 0.5 g PVP: (a-c) reaction for 10 mins, (d-f) reaction for 30 mins, (g-i) reaction for 60 mins

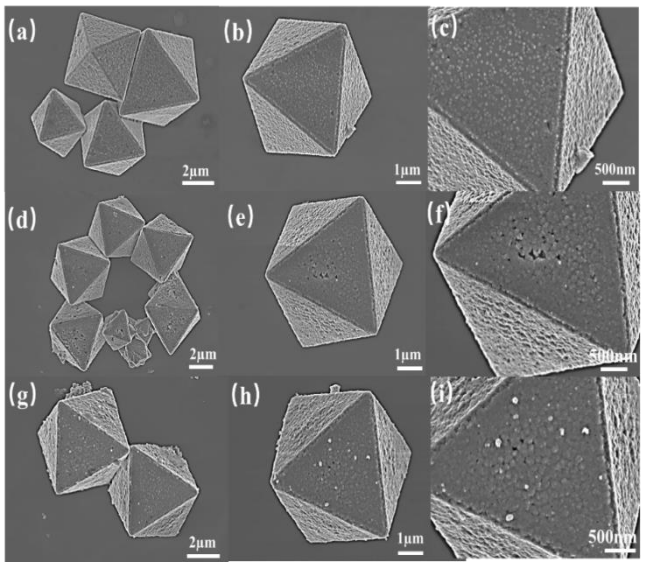

Figure 7: SEM diagram of Cu2O-Cu heterostructure prepared by adding 1 g PVP: (a-c) reaction for 10 mins, (d-f) reaction for 30 mins, (g-i) reaction for 60 mins

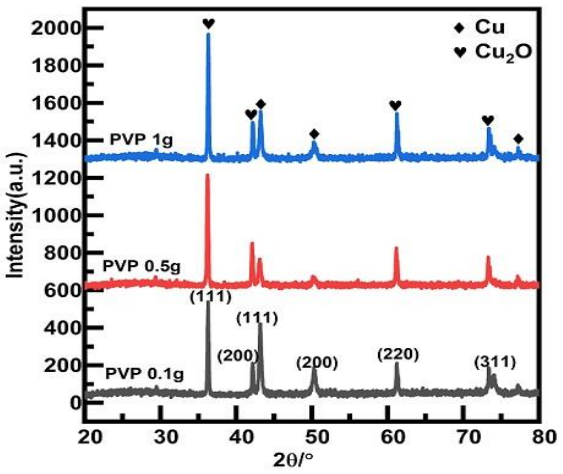

Figure 8: XRD diagram of Cu2O-Cu heterostructures prepared by adding different amounts of PVP and reacted at 60 ℃ for 60 mins

3.3 Effect of CTAB on Cu2O-Cu heterostructures

As shown in Figure 9, when 0.1 g of CTAB surfactant was added, the number of surface particles on the sample prepared by the reaction for 10 mins decreased compared with no surfactant, but after the reaction time increased to 30 mins and 60 mins, the particle size of Cu nanoparticles became significantly larger. However, as shown in Figure 10 and Figure 11, when the addition amount of CTAB was increased to 0.5 g and 1.0 g, the particle size of Cu nanoparticles became smaller again, which was consistent with the performance without CTAB. Therefore, the addition of a small amount of CTAB can increase the particle size of Cu nanoparticles in the Cu2O-Cu heterostructure. The XRD results shown in Figure 12 also show that the addition of CTAB does not change the phase of the product.

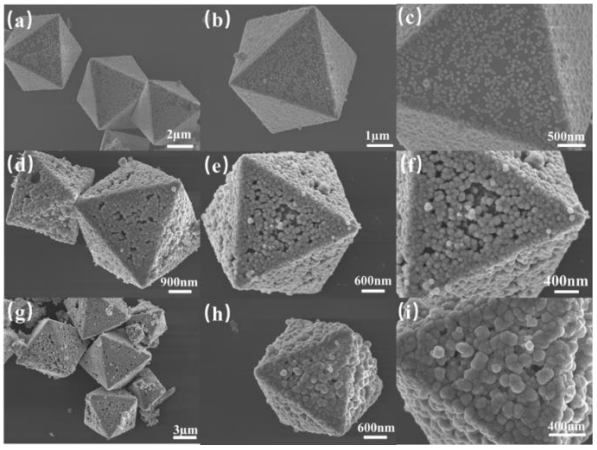

Figure 9: SEM images of Cu2O-Cu heterostructures prepared by adding 0.1 g CTAB: (a-c) reaction for 10 mins, (d-f) reaction for 30 mins, (g-i) reaction for 60 mins

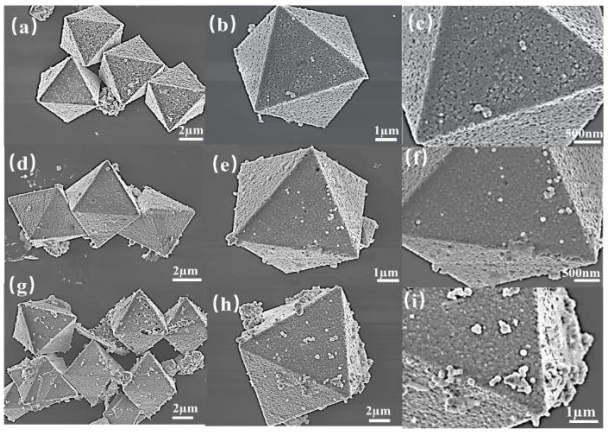

Figure 10: SEM images of Cu2O-Cu heterostructures prepared by adding 0.5 g CTAB: (a-c) reaction for 10 mins, (d-f) reaction for 30 mins, (g-i) reaction for 60 mins

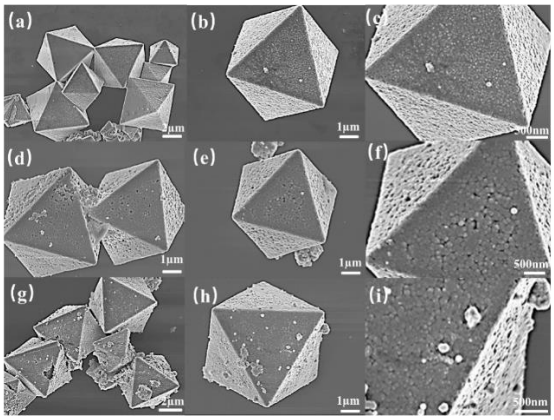

Figure 11: SEM diagrams of Cu2O-Cu heterostructures prepared by adding 1 g CTAB: (a-c) reaction for 10 mins, (d-f) reaction for 30 mins, (g-i) reaction for 60 mins

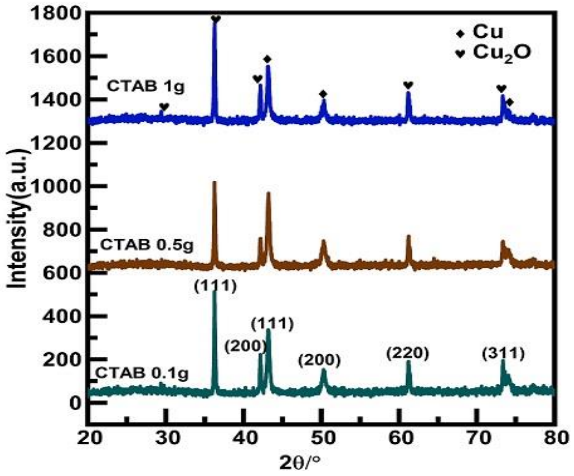

Figure 12: XRD diagram of Cu2O-Cu heterostructures prepared by adding different amounts of CTAB and reacting at 60 °C for 60 mins

3.4 Effect of SDS on Cu2O-Cu heterostructures

As shown in Figure 13 and Figure 14, after adding 0.1 g and 0.5 g of anionic surfactant SDS, the Cu nanoparticles on the surface of the Cu-Cu2O heterostructure become finer and more uniform than when no active agent was added, and the wrapping property also becomes better. As shown in Figure 15, when the dose of SDS is increased to 1.0 g, in the Cu-Cu2O heterostructure reacted for 10 mins, the particle size of the Cu nanoparticles is further reduced, and almost has shown a dense state, and when the reaction time is increased to 30 mins and 60 mins, the shell layer of Cu particles formed also appears denser and uniform. As shown in Figure 16, the XRD detection results also show that the addition of surfactant SDS does not generate new substances, but still reduces Cu2O to Cu nanoparticles in situ.

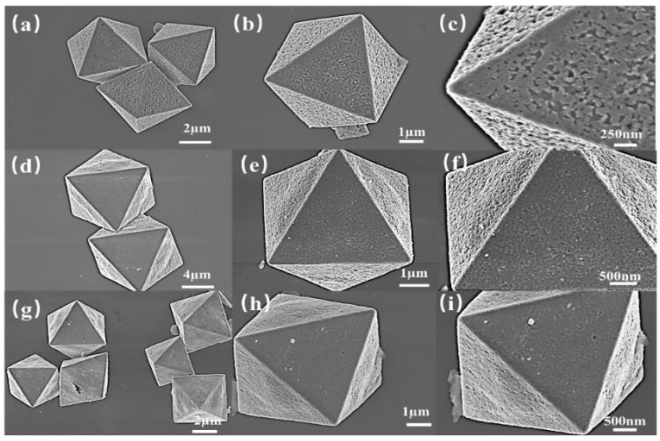

Figure 13: SEM images of Cu2O-Cu heterostructures prepared by adding 0.1 g SDS: (a-c) reaction for 10 mins, (d-f) reaction for 30 mins, (g-i) reaction for 60 mins

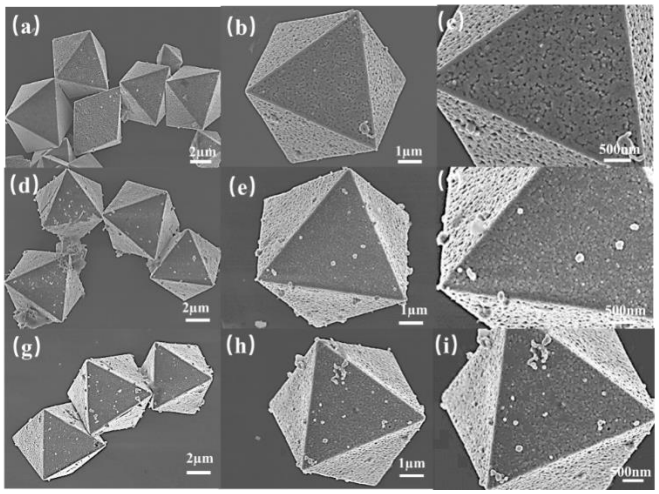

Figure 14: SEM images of Cu2O-Cu heterostructures with 0.5 g SDS: (a-c) reaction for 10 mins, (d-f) reaction for 30 mins, (g-i) reaction for 60 mins

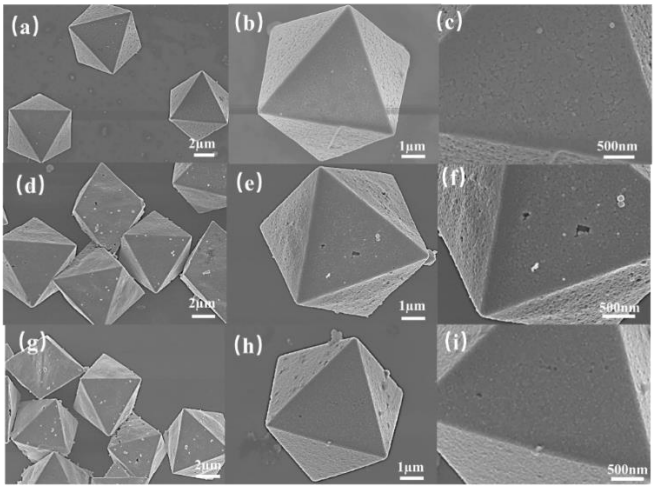

Figure 15: SEM images of Cu2O-Cu heterostructures prepared by adding 1 g SDS: (a-c) reaction for 10 mins, (d-f) reaction for 30 mins, (g-i) reaction for 60 mins

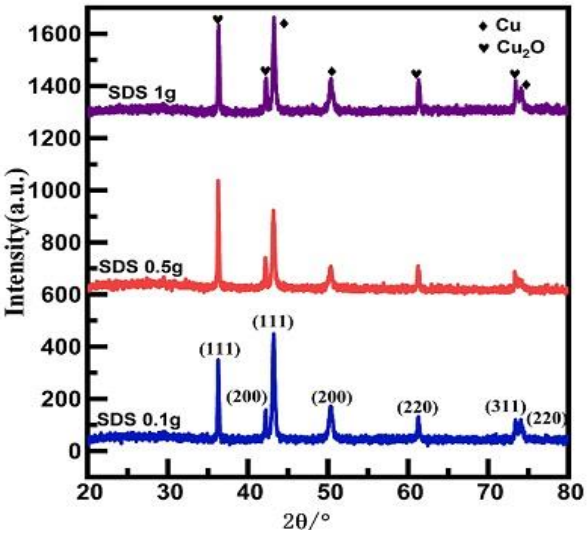

Figure 16: XRD diagram of Cu2O-Cu heterostructures prepared by adding different amounts of SDS and reacting at 60 °C for 60 mins

4. Conclusion

In this paper, the Cu2O powder was prepared first, the monovalent Cu was reduced to zero-valent Cu by the reduction of glucose. Then different amounts of surfactants PVP, CTAB, and SDS were added to achieve the preferential growth of nano-Cu at different positions of octahedral Cu2O. The addition of PVP has the main effect on the edge position of the

octahedral Cu2O particles, which will hinder the in-situ reduction reaction of Cu2O to Cu nanoparticles at the edge position of the octahedral Cu2O particles, so that there is almost no in-situ growth of Cu particles at the edge of the Cu2O-Cu heterostructure. The addition of CTAB does not significantly change the distribution of Cu particles, but it will increase the particle size of Cu particles. The addition effect of SDS is the opposite of the former two, not only will the particle size of nano-Cu in the Cu2O-Cu heterostructure be smaller, but also it will grow preferentially and aggregate on the octahedral Cu2O edge.

ACKNOWLEDGMENTS

This work was supported by the Key Research and Development Program (Talents Introduction Project) of Ningxia (No. 2022BSB03055), the Fundamental Research Funds for the Central Universities, North Minzu University (No. 2021KYQD02), and the Innovation Training Project for College Students (No. 202311407022).

REFERENCES

Abd-Elkader, O.H., and Deraz, N.M., 2013. Synthesis and Characterization of New Copper based Nanocomposite. International Journal of Electrochemical Science, 8 (6), Pp. 8614-8622. doi: 10.1016/S1452-3981(23)12913-0.

Badry, R., Nada, N., El-Nahass, M.M., Elhaes, H., and Ibrahim, M.A., 2024. Enhanced Sensing Performance of Carboxymethyl Cellulose Sodium to Hydrogen Sulphide Gas and Methylene Blue Dye by Constructing CuO@ZnO Core/Shell Heterostructure: A DFT/TD-DFT Study. Optical and Quantum Electronics, 56 (3), Pp. 326. doi: 10.1007/s11082-023-05942-y.

Balakrishnan, K.P., Senthilkumar, K.K., Gokila, N., Thangavelu, R.K.R., Annamalai, P.K., and Raghava, R.B.T.S., 2024. Surfactant Assisted Tuning of Electrical Conductivity, Electromagnetic Interference Shielding Effectiveness, Wetting Properties of Poly (Lactic Acid)-Expanded Graphite-Magnetite Nanocube Hybrid Bio-Nanocomposites. European Polymer Journal, 214, Pp. 113135. doi: 10.1016/j.eurpolymj.2024.113135.

Chachvalvutikul, A., Luangwanta, T., Pattisson, S., Hutchings, G.J., and Kaowphong, S., 2021. Enhanced Photocatalytic Degradation of Organic Pollutants and Hydrogen Production by A Visible Light–Responsive Bi2WO6/ZnIn2S4 Heterojunction. Applied Surface Science, 544, Pp. 148885. doi: 10.1016/j.apsusc.2020.148885.

Choi, J., and Yoon, S., 2022. Structural Information of Nanosized Iron Oxide Clusters Serendipitously Poses the Solution of Long-Standing Problems on Nanomaterials: Intra/Inter Surfactant and Core-Surfactant Interaction. Bulletin of the Korean Chemical Society, 43 (2), Pp. 299-304. doi: 10.1002/bkcs.12456.

Gore, V.M., Nagare, T.T., Desai, M.A., and Sartale, S.D., 2024. Enhancing Photoelectrochemical Performance of ZnO Nanorods by Forming ZnO–ZnS Heterostructure via Ion-Exchange Process. Journal of Materials Science: Materials in Electronics, 35 (17), Pp. 1145. doi: 10.1007/s10854-024-12764-5.

Hamdani, I.R., and Bhaskarwar, A.N., 2022. Tuning of the Structural, Morphological, Optoelectronic and Interfacial Properties of Electrodeposited Cu2O Towards Solar Water-Splitting by Varying the Deposition pH. Solar Energy Materials and Solar Cells, 240, Pp. 111719. doi: 10.1016/j.solmat.2022.111719.

Javaid, S., Farrukh, M.A., Muneer, I., Shahid, M., Khaleeq-ur-Rahman, M., and Umar, A.A., 2015. Influence of Optical Band Gap and Particle Size on the Catalytic Properties of Sm/SnO2–TiO2 Nanoparticles. Superlattices and Microstructures, 82, Pp. 234-247. doi: 10.1016/j.spmi.2015.01.038.

Kempasiddaiah, M., Samanta, R., Panigrahy, S., Trivedi, R.K., Chakraborty, B., and Barman, S., 2024. Electrochemical Reconstruction of a 1D Cu (PyDC) (H2O) MOF into in Situ Formed Cu-Cu2O Heterostructures on Carbon Cloth as an Efficient Electrocatalyst for CO2 Conversion. Nanoscale, 16 (21), Pp. 10458-10473. doi: 10.1039/D4NR00824C.

Kociołek-Balawejder, E., Gibas, A., Baszczuk, A., Jasiorski, M., and Jacukowicz-Sobala, I., 2023. Transformation of CuO and Cu2O Particles into CuxS within the Polymeric Matrix of Anion Exchangers, and its Structural and Morphological Implications. Reactive and Functional Polymers, 192, Pp. 105734. doi: 10.1016/j.reactfunctpolym.2023.105734.

Li, X. Chen, J. Wang, Y. Liu, N. Liu, C. Du, P. Xia, Y. He, S., 2024. Photocatalytic Reaction Pathways and Mechanisms Investigation for Effective Organic Pollution Degradation via in-situ Construction of BiOCl/UiO66-NH2 Heterostructure. Applied Surface Science, 669, Pp. 160537. doi: 10.1016/j.apsusc.2024.160537.

Liyanaarachchi, U.S., and Fernando, C.A.N., 2013. Photoelectrochemical Characteristics of CuO Free p-Cu2O Thin Films Prepared by Easy Fabrication Method. Invertis Journal of Renewable Energy, 3 (4), Pp. 206-211.

Ma, B., Kong, C., Lv, J., Zhang, W., Guo, J., Zhang, X., Yang, Z., and Yang, S., 2018. Controllable in-situ Synthesis of Cu-Cu2O Heterostructures with Enhanced Visible-light Photocatalytic Activity. Chemistry Select, 3 (38), Pp. 10641-10645. doi: 10.1002/slct.201802880.

Malik, M.K.T., Fakhr-e-Alam, M., Ullah, F., Ramay, S.M., and Saleem, M., 2024. A Comparative Study of DFT and Experimental Investigations for Exploring the Effect of Ti Doping on the Electronic, Structural, and Optical Properties of Cu2O. Physica B: Condensed Matter, 686, Pp. 416090. doi: 10.1016/j.physb.2024.416090.

Mani, S., Jang, J.I., Ketterson, J.B., and Park, H.Y., 2009. High-Quality Cu2O Crystals with Various Morphologies Grown by Thermal Oxidation. Journal of Crystal Growth, 311 (14), Pp. 3549-3552. doi: 10.1016/j.jcrysgro.2009.05.006.

Murzin, S.P., 2023. Formation of ZnO/CuO Heterostructures Based on Quasi-One-Dimensional Nanomaterials. Applied Sciences, 13 (1), Pp. 488. doi: 10.3390/app13010488.

Özdal, T., and Kavak, H., 2020. Fabrication and Characterization of ZnO/Cu2O Heterostructures for Solar Cells Applications. Superlattices and Microstructures, 146, Pp. 106679. doi: 10.1016/j.spmi.2020.106679.

Uthirakumar, P., Son, H., Dao, V., Lee, Y., Yadav, S., and Lee, I.H., 2024. Accelerating Photoelectrochemical CO2RR Selectively of C2+ Products by Integrating Ag/Pd Cocatalysts on Cu/Cu2O/CuO Heterojunction Nanorods. Journal of Environmental Chemical Engineering, 12 (2), Pp. 112442. doi: 10.1016/j.jece.2024.112442.

Xiong, L., Huang, S., Yang, X., Qiu, M., Chen, Z., and Yu, Y., 2011. p-Type and n-Type Cu2O Semiconductor Thin Films: Controllable Preparation by Simple Solvothermal Method and Photoelectrochemical Properties. Electrochimica Acta, 56 (6), Pp. 2735-2739. doi: 10.1016/j.electacta.2010.12.054.

Yoon, H., Kim, H., Matteini, P., and Hwang, B., 2022. Research Trends on the Dispersibility of Carbon Nanotube Suspension with Surfactants in Their Application as Electrodes of Batteries: A Mini-Review. Batteries, 8 (12), Pp. 254. doi: 10.3390/batteries8120254.

Zhao, K., Tang, J., Tian, S., Li, X., Yang, H., Wang, X., and Zeng, D., 2023. Enhanced Room-Temperature NH3 Sensing Properties of Cu2O Concave Octahedron/ CNTs Heterostructured Hybrid via Efficient Charge Transfer. Sensors and Actuators B: Chemical, 385, Pp. 133724. doi: 10.1016/j.snb.2023.133724.